

A Study on Second Mode Stress Intensity Factor (K_{II}) of Cracked Plates Under Compression Load

Nathera Abdual Hassan Saleh

Basrah University, Engineering College , Mechanical Department
e-mail : Nathera1971@yahoo.com

Abstract

A two-dimensional finite element method for analysis and determination of second mode stress intensity factor (K_{II}) of several crack configurations in plates under uniaxial compression is presented in this study. Various cases including diagonal crack (i.e. corner crack, central crack as well as at different locations on the diagonal) and central kinked crack are investigated with different crack's length, orientation and location. The influence of the contact between two crack surfaces is taken into account by applying contact element procedure with desired friction coefficient. The stress intensity factor is calculated by a crack surface displacement extrapolation technique. From the obtained results of the analysis it is found that, the corner cracked plates more dangerous than the other cracked plates, since it has the highest stress intensity factor. Also, the length and orientation of the kinked crack have significant effects on the stress intensity factor. The results of this investigation is illustrated graphically, exposing some novel knowledge about the stress intensity factor and its dependence on crack configuration.

دراسة الطور الثاني لمعامل شدة الإجهاد لصفائح متشققة تحت حمل الانضغاط

نظيره عبدالحسن صالح

جامعة البصرة - كلية الهندسة - قسم الهندسة الميكانيكية

الملخص :

قدمت في هذه الدراسة طريقة العناصر المحددة ثنائية البعد للتحليل و حساب الطور الثاني لمعامل شدة الإجهاد (K_{II}) لعدة أشكال من الشق في الصفائح تحت الانضغاط باتجاه واحد. تم بحث حالات مختلفة من الشق القطري (شق زاوي ، شق مركزي، بالإضافة إلى عند أي موقع من القطر) و شق مركزي متفرع لحالات مختلفة من طول ، ميلان و موقع الشق. تأثير التماس بين سطحي الشق أخذ بنظر الاعتبار بالحساب بتطبيق أسلوب العناصر المتماصة مع معامل احتكاك مناسب. معامل شدة الإجهاد حسب باستخدام تقنية استقراء الإزاحة عند سطح الشق. من النتائج المستحصلة من التحليل بينت بأن الصفائح المشققة زواياً أكثر خطورة من الصفائح المشققة الأخرى، لأنها تمتلك أعلى معامل شدة الإجهاد. كذلك طول و ميلان الشق المتفرع لهم تأثير هام على معامل شدة الإجهاد. نتائج هذا البحث وضحت تخطيطياً لعرض بعض المعرفة الجديدة حول معامل شدة الإجهاد و اعتماده على شكل الشق.

1. Introduction

In practical engineering problems, different types and numbers of cracks are often randomly distributed and encountered in the structure components under various loading and boundary conditions. So, the strength of a structure could be severely affected by the presence of crack and the defects are unavoidable in a cost effective manufacturing process. In most of the structures, cracks may be located or developed during the service in the zones of stress concentration and the crack may be large enough so that the crack-tip may be closer to a boundary. The crack may grow to cause structure failure due to low stress, which acts to a structure. Stress intensity factor (SIF) is a most important single parameter in fracture mechanics, which can be used to examine if a crack, would propagate in a cracked structure under particular loading condition, i.e. it controls the stability of the crack. For relatively simple components and loadings, SIF can be calculated very easily, but problem might arise when one is dealing with complicated cracked structures. Regarding this problem, numerical analysis is one of the powerful means to provide some parameters for examining the stability of the cracked structures (i.e. SIF). A large number of numerical techniques are available in the literature for estimation of the stress intensity factors. Many of the widely used techniques were reviewed in Refs. [1–4]. In addition, the SIF solutions of large number of simple cracked configurations are compiled in various handbooks [5,6].

In the majority of previous studies are focused on the mechanisms of crack initiation and propagation of opening (mode I) cracks, i.e. tensile loading. However cracks can be subjected to compression load and such cracks can pose a potential risk just as cracks under tensile loading. The crack is closed under compression load

in some cases and this state involves additional features compared to analyses restricted to open cracks because of the normal and tangential (frictional) forces arising on the crack surfaces in contact, which strongly influences the SIF as well as the stress and the displacement fields at the crack tip and must be considered. A contact between crack surfaces can be analyzed as a general contact mechanics problem of two elastic bodies [7]. Due to the elimination of crack surface opening, the growth of cracks with crack surface contact is in the shear mode (or mode II under in plane loading conditions).

Many researchers have attempted to extend the fracture mechanics approach to treat various engineering problems involving cracks with frictional contact, but mainly concerned with brittle fracture in materials such as concrete, rock structures and geophysics using different solution techniques (i.e. analytical, numerical and experimental) under uniaxial or biaxial compression to investigate SIF of straight, kinked and wing cracks [8-15]. Thus, to the knowledge of the author, there are few studies that address the simulation of crack contact problems in metal plates.

Zhu et al.[16-18] presented a boundary collection method based on a set of complex stress functions to investigate SIF for a mixed mode crack with various plates containing center cracks of different angular orientation under compression and shear loads. Also, they studied influence of coefficient of friction on SIF under biaxial compression load [18]. Besides, the boundary integral method was employed by some authors to deal with various crack configurations (i.e. single and multiple cracks) considering frictional contact analysis of SIF determination [19,20]. Chau and Wang [19] used it for the problem of two-dimensional elastic solids containing one, two and an infinite array of central inclined frictional cracks under far field

biaxial compression. While, Tsung and Wen [20] analyzed by this method finite plates containing cracks of linear, curved and kinked types under uniaxial compression.

Review of the literature shows that the finite element method is perhaps the most commonly used numerical method to model crack contact problems in determination of the stress intensity factors and related matters. Isaksson and Stahle [21,22] investigated the problem for straight stationary crack with a small incipient kink under combined hydrostatic pressure and pure shear assuming homogenous Coulomb friction between crack surfaces in contact. They derived a theoretical solution for prediction of the direction of initiated crack growth depend on evaluation of stresses near crack tip [21] and employed this solution for studying crack opening displacement [22], as well as the solution validation is examined in a finite element analysis. The behavior of a central slant crack in a plate for plane strain state was investigated by Hammouda et al. [23-26]. They discussed many situations in their works as : the effect of crack surface friction on mode II SIF in uniaxial compression [23], the evaluation of the modes II and I SIFs in uniaxial compression [24] and biaxial (i.e. tension- compression) [25] as well as the determination of the crack initiation angle by calculating the normal and tangential crack tip relative displacement in biaxial (i.e. tension-compression) [26], of a shortly kinked slant central crack with frictional surfaces.

Recently, Xian et. al. [27] studied crack extension resulting from a closed crack in compression using a modified maximum tensile stress criterion with the singular and non-singular terms. They determined kinking angle at the onset of crack growth by a two parameter field involving the mode-II SIF and T -stresses.

As can be seen from the above-mentioned works, most of the previous studies are focused on stationary cracks at

one place, edge [21,22] or central [16-18,23-27] and for constant length of shortly kinked cracks[26]. So, the present study investigates the effects of the crack location and the crack kink extension on the second mode SIF (K_{II}) in addition to crack size and crack orientation with frictional contact crack surfaces by using finite element analysis (ANSYS Software).

2- Theoretical Background

According to fracture mechanics, stress field at the tip of mixed mode I-II crack shown in figure (1) is [5,6]

$$\begin{Bmatrix} \sigma_{xx} \\ \sigma_{yy} \\ \tau_{xy} \end{Bmatrix} = \frac{K_I}{\sqrt{2\pi r}} \cos \frac{\theta}{2} \begin{Bmatrix} 1 - \sin \frac{\theta}{2} \sin \frac{3\theta}{2} \\ 1 + \sin \frac{\theta}{2} \sin \frac{3\theta}{2} \\ \sin \frac{\theta}{2} \cos \frac{3\theta}{2} \end{Bmatrix} \dots(1) \\ + \frac{K_{II}}{\sqrt{2\pi r}} \begin{Bmatrix} -\sin \frac{\theta}{2} \left(2 + \cos \frac{\theta}{2} \cos \frac{3\theta}{2} \right) \\ \sin \frac{\theta}{2} \cos \frac{\theta}{2} \cos \frac{3\theta}{2} \\ \cos \frac{\theta}{2} \left(1 - \sin \frac{\theta}{2} \sin \frac{3\theta}{2} \right) \end{Bmatrix}$$

where K_I , K_{II} denote the mode-I and mode-II stress intensity factors, characterizing the singular behavior caused by the normal and shear components of stress at the crack surfaces, respectively. In the above expressions, r and θ are local polar coordinates with the origin located at the crack tip, (Figure (1)). For an opening inclined crack at (β) of finite length $2a$ embedded in an infinite elastic plane subjected to tensile loading (σ) at infinity the resolved normal (σ_{yy}) and shear stresses (τ_{xy}) are given by figure (1b):

$$\sigma_{yy} = \sigma \sin^2 \beta \dots \dots \dots (2a)$$

$$\tau_{xy} = \sigma \sin \beta \cos \beta \dots \dots \dots (2b)$$

the mode I and mode II stress intensity factors are given by

$$K_I = \sigma_{yy} \sqrt{\pi a} = \sigma \sqrt{\pi a} \sin^2 \beta \dots \dots \dots (3a)$$

$$K_{II} = \tau_{xy} \sqrt{\pi a} = \sigma \sqrt{\pi a} \sin \beta \cos \beta \dots \dots \dots (3b)$$

In most cases, note that in compression, there is no equivalent to crack opening, and thus, if the tensile stress is replaced by a compressive stress, there is no mode I SIF. However, the material can still fail by shear, and in the absence of friction the mode II SIF is still that given by (3), which is the result normally quoted for the SIF for a crack in compression. With frictional crack surfaces, the resolved shear stress (τ_{xy}) on the crack faces causes the cracks to slide is resisted by the frictional stress (τ_f) induced by the normal stress (σ_{yy}) on the crack surfaces, figure (1c). When the applied resolved shear stress exceeds the frictional stress, the net resolved shear stress distribution along the crack face acts as the driving force for the crack to undergo sliding. This frictional sliding gives rise to tensile stress fields at the tips of the crack. The frictional shear stress, which oppose sliding of crack surfaces, is related to the pressure on the crack face through Coulomb friction law [12,27]:

$$\tau_f = \mu \sigma_{yy} = \mu \sigma \sin^2 \beta \dots \dots \dots (4)$$

where μ is the coefficient of friction. Then the effective shear stress (τ_{eff}) on the surface is

$$\begin{aligned} \tau_{eff} &= \tau_{xy} - \tau_f \\ \tau_{eff} &= \sigma \sin \beta \cos \beta - \mu \sigma \sin^2 \beta \\ \tau_{eff} &= \sigma \sin \beta (\cos \beta - \mu \sin \beta) \dots \dots \dots (5) \end{aligned}$$

The SIF at the crack tip is the mode II factor :

$$\begin{aligned} K_{II} &= \tau_{eff} \sqrt{\pi a} \\ K_{II} &= \sigma \sin \beta (\cos \beta - \mu \sin \beta) \sqrt{\pi a} \dots \dots \dots (6) \end{aligned}$$

Consequently, if the crack advances when certain fracture criteria are satisfied it may be kinked from main crack. The kinked cracks are in general asymmetric, unequal, and arbitrarily oriented and located [10]. Theoretical models of frictional kinked crack are often based on compressive brittle failure [9-11]. For example, Nemat-Nasser and Horii [cited in Ref.26] suggested an analytical solutions for the mode I and mode II SIF, respectively K_I^α and K_{II}^α of an infinitesimal kink extending from a slant crack with frictional surfaces in a compressed infinite plate, see Figure (2) :

$$K_I^\alpha = 0.75 K_{II}^0 [\sin(\alpha/2) + \sin(3\alpha/2)] \dots \dots \dots (7a)$$

$$K_{II}^\alpha = 0.25 K_{II}^0 [\cos(\alpha/2) + 3 \cos(3\alpha/2)] \dots \dots \dots (7b)$$

Where α is the kink crack angle and K_{II}^0 the SIF of mode II as given in equation (6).

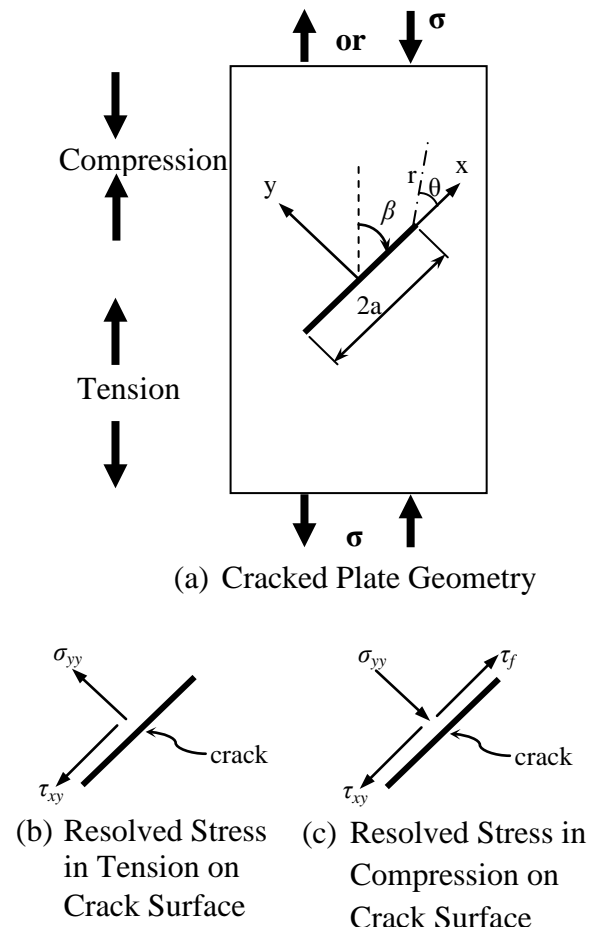


Figure (1) Schematic of a Plate With an Inclined Central Crack Under Tension or Compression

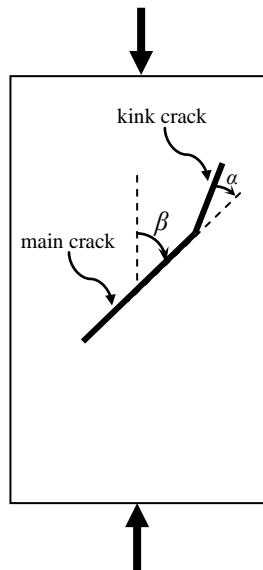


Figure (2) Schematic of a Plate With an Inclined Main Crack and Kink Crack Under Compression

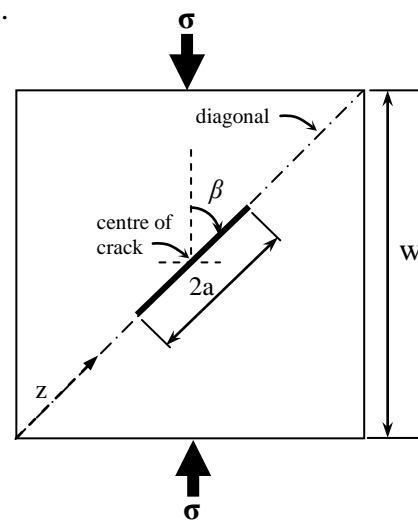
3. Two-Dimensional Finite Element Modeling Issues

There are several issues must be addressed during the calculation of SIF of cracked plates under compression using finite elements analysis which can be summarized in the following sections.

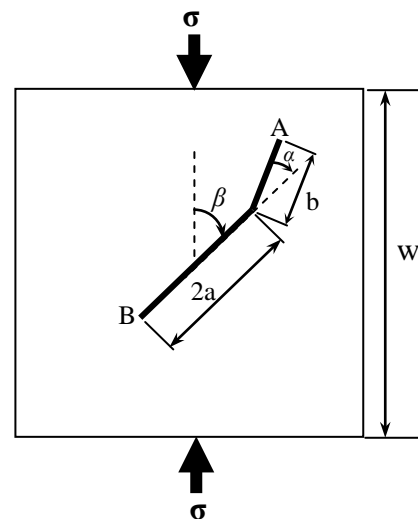
3.1 Model Description

This section presents description of the case studies under investigation. Two case studies of cracked square plates for plane strain state have been selected, First case: Diagonal cracked plate with different crack location in diagonal-direction and Second case: Central cracked plate with kinked crack, the configurations of the cracked plate can be defined according to figure (3). The studied dimensionless geometric parameters are as follows: relative crack's length ($2a/w = 0.1 - 0.5$), crack orientation ($\beta = 0^\circ - 75^\circ$), relative crack location ($z/d = 0.1, 0.2, 0.3, 0.5$) where d : is the

diagonal length and z : the distance from plate corner to the crack centre, relative kinked crack length ($b/a = 0.05-0.25$) and kinked crack angle ($\alpha = 15^\circ-75^\circ$). In first case, the value of $z/d=0$ corresponds to the corner cracked plate, also when $z/d=0.5$ this represents central cracked plate. The plate material considered is supposed to be linear elastic and isotropic with Young's modulus : $E=200\text{GN/m}^2$ and Possion's ratio $\nu = 0.3$.



(a) Diagonal crack



(b) Central crack with kinked crack

Figure (3) Cracked Square Plate with Crack Type Details

Finite element analysis of all case studies is carried out using general purpose finite element software ANSYS ver.11. Eight-node elements (PLANE82) were

chosen from ANSYS element library for meshing procedure. This element is defined by eight nodes having two degrees of freedom at each node: translations in the nodal x and y directions. It provides more accurate results for mixed (quadrilateral-triangular) automatic meshes and can tolerate irregular shapes without as much loss of accuracy. The element has plasticity, creep, swelling, stress stiffening, large deflection, and large strain capabilities [adopts from ANSYS help]. Figure (4) shows the typical finite element meshes employed in the present work.

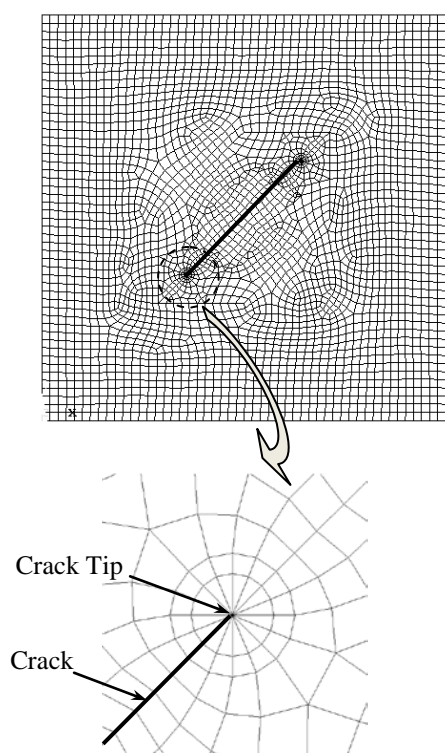


Figure (4) Finite Element Mesh Sample
For a Cracked Plate With Crack-tip
Mesh Detail

3.2 Modeling of Crack With Surface Contact

The most important region in a fracture model is the region around the edge of the crack (i.e. crack tip). To pick up the singularity around the crack, the crack faces should be coincident, and the elements

around the crack tip (or crack front) should be quadratic, with mid-side nodes placed at the quarter points. Such elements are called singular elements or quarter point elements which are distributed in a spider web pattern at a crack tip, figure(4). This feature can be achieved by using PLANE82 element. In order to simulate the contact between the crack surfaces in the two-dimensional modeling, a surface-to-surface contact, which consists of contact elements (CONTA172) and target segment elements (TARGE1169), is used on the interfaces between the crack surfaces. Coulomb friction model was used as it is supported by ANSYS with friction coefficient (μ) of 0.25.

3.3 Calculation of SIF using finite elements

It well known that the SIF may be computed in numerous techniques by using finite element analysis, which can be divided into three groups:

- (i) Methods based on the values of the stresses or displacement in the region near the crack tip (i.e. the method of extrapolation of the apparent SIF).
- (ii) Methods based on the calculation of the strain energy released at a small stable growth of the crack (i.e. the method of the energy release rate and the method of the virtual extension).
- (iii) Methods based on the computation of contour integrals used in fracture mechanics (i.e. the method of the J integral).

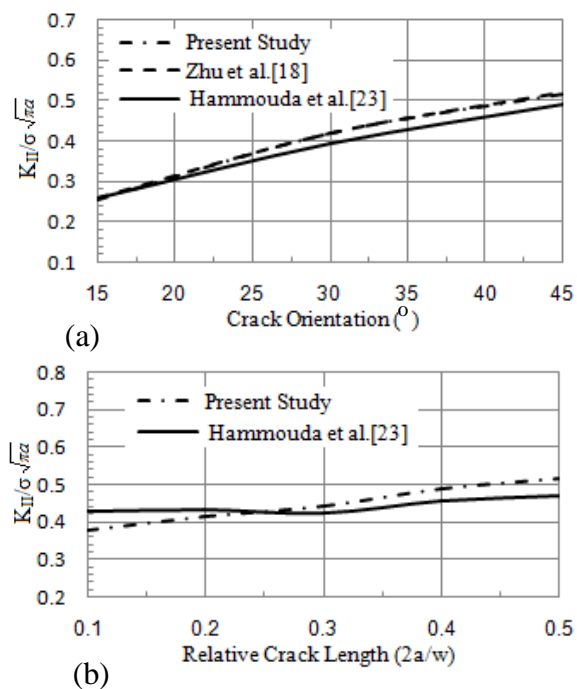
All these methods can use both conventional or singular elements. The most usual method is to equate the finite element representation for displacements near the crack tip with those expressing the behavior of displacements from the fracture mechanics point of view. Consequently, the displacement extrapolation method is employed to get SIF throughout this work by utilizing (KCALC) command in ANSYS catalogue of commands.

3.4 Verification of The Finite Element Model

It is essential for any finite element model to verify whether the results obtained match with other models. This substantiates that the model is realistic enough to capture the rest of the outcomes. Therefore, the comparison between previous published numerical simulation of the normalized mode II SIF (i.e. $K_{II}/\sigma \sqrt{\pi a}$) reported by Zhu Z. et. al. [18] as well as Hammouda et. al. [23] and the present numerical simulation results is executed, figure (5). The verification is conducted for the two center cracked plates configuration with (i) $2a/w = 0.1$, $\beta = (15^\circ-45^\circ)$, $\mu = 0$ and (ii) $2a/w = 0.1-0.5$, $\beta = 45^\circ$, $\mu = 0.125$. At first, the convergence characteristic of the proposed model is explored. Thus, the quality of the final pattern and density of the finite element mesh have been accepted after several convergence tests in which the mesh density and element shapes are varied with that case studies. To compare the results of the present study with the published data, percent difference is calculated as :

$$\text{difference\%} = \left| \frac{\text{computed value} - \text{reference value}}{\text{reference value}} \right| \times 100$$

where the “computed value” refers to the value obtained using the proposed model, and “reference value” is the available numerical value (i.e. Ref. [18] or [23]). It is seen that the maximum difference is less than 0.35% and 2.65% among Zhu Z. et. al. [18] results and Hammouda et. al. [23] results respectively, figure(5a). As well as, the results would differ less than 4.6% from those of by Hammouda et. al. [23], figure(5b). Thus, it be seen from figure(5) that, there is a good agreement between current results and previous results.



Figure(5) Finite Element Model Verification

4. Results and Discussion

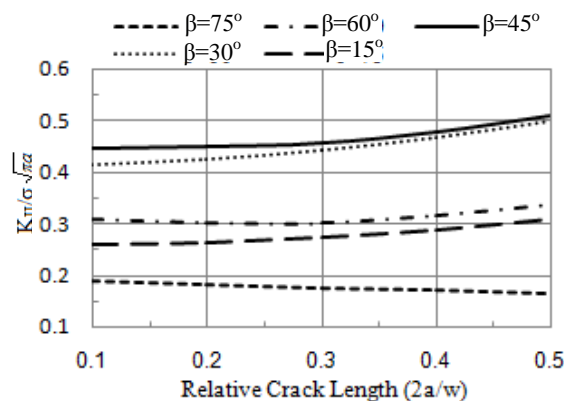
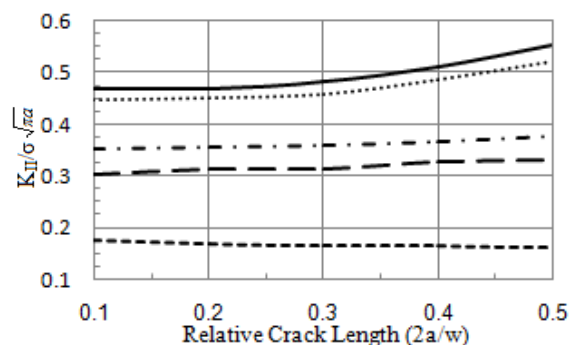
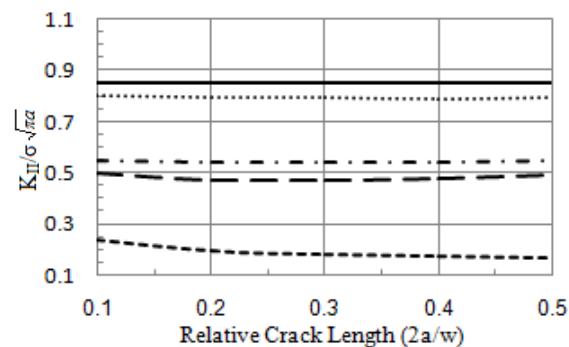
The effects of different crack parameters described in section 3.1 on the normalized mode II SIF (i.e. $K_{II}/\sigma \sqrt{\pi a}$) of the two selected cases studies are analyzed and the results are discussed in this section.

4.1 Diagonal Cracked Plates

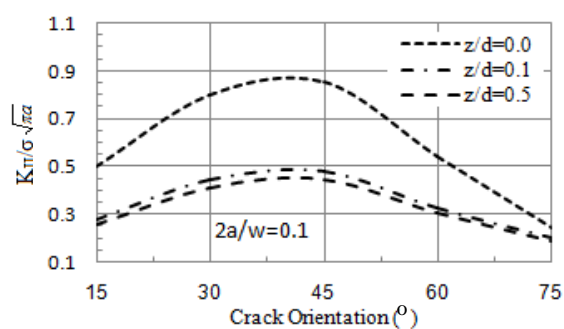
Figure (6a - 6c) shows the variation of $K_{II}/\sigma \sqrt{\pi a}$ with relative crack length ($2a/w$) for different crack orientation in the cases of central crack ($z/d=0.5$) , diagonal crack ($z/d=0.3$) and corner crack ($z/d=0$) respectively. Generally, it can be noted from this figure that as crack orientation increases from 15° to 45° the value of $K_{II}/\sigma \sqrt{\pi a}$ increases and then decreases when crack orientation increases from 60° to 75° for all crack lengths of the three cases is agreement to the results reported in [23]. This behavior may be attributed to the relation between loading direction and

crack face. Since the crack orientations relatively small, the loading direction approaches to be parallel to the crack face. While, it approaches to be normal to the crack face as the crack orientation becomes large. Furthermore, according to figure(6a, 6b) the variation of $K_{II}/\sigma\sqrt{\pi a}$ is more sensitive to the crack orientation especially at 30° or 45° with growing crack length than the other crack orientation for first two cases. Whereas, it is slightly sensitive (i.e. almost unchanged) to crack orientation for the third case, figure(6c). Except at 75° it decreases as crack length raises for all cases.

Figure(7) illustrates the sensitivity of the $K_{II}/\sigma\sqrt{\pi a}$ to the crack location on the diagonal of the plate to assess the effect of the crack location upon $K_{II}/\sigma\sqrt{\pi a}$. The results showed that the variation in $K_{II}/\sigma\sqrt{\pi a}$ with different crack length and orientation were very similar in behavior and for brevity, only some cases have been selected. The case of corner crack has always higher values of $K_{II}/\sigma\sqrt{\pi a}$ than the other cases. The reason behind this performance mentioned where the presence of the crack at the corner of the plate can significantly be effect by loading state leading to affected in shear stress and consequently in K_{II} . Figure(8) demonstrates graphically enhancement the findings discussed here.

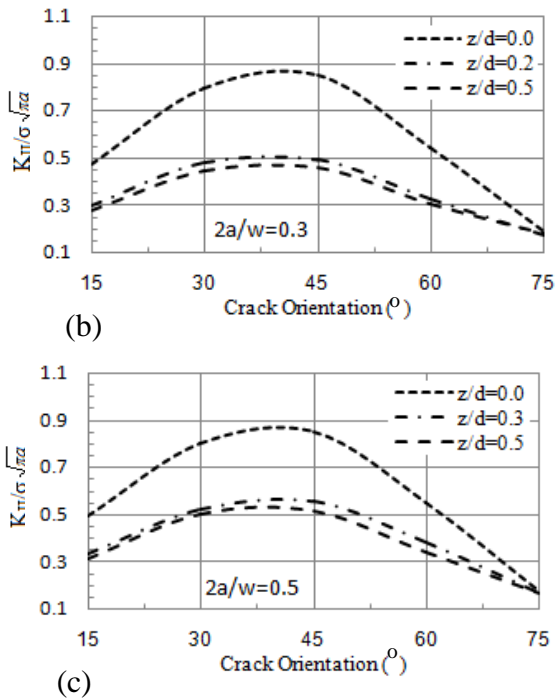
(a) Centre crack ($z/d=0.5$)(b) Diagonal crack ($z/d=0.3$)(c) Corner crack ($z/d=0$)

Figure(6) Normalized Mode II SIF Versus Relative Crack Length for Different Crack Orientation

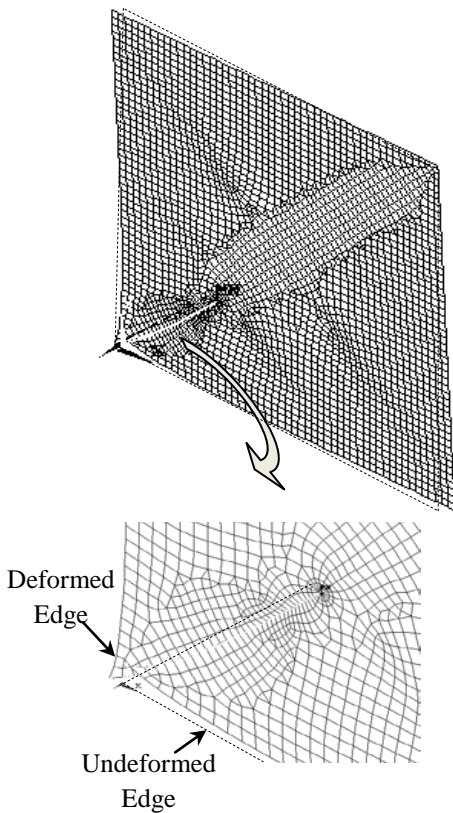


(a)

(Continued)



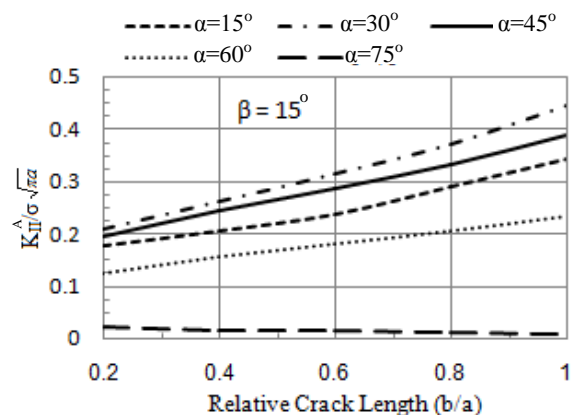
Figure(7) Normalized Mode II SIF Versus Crack Orientation for Different Relative Crack Length and Crack location



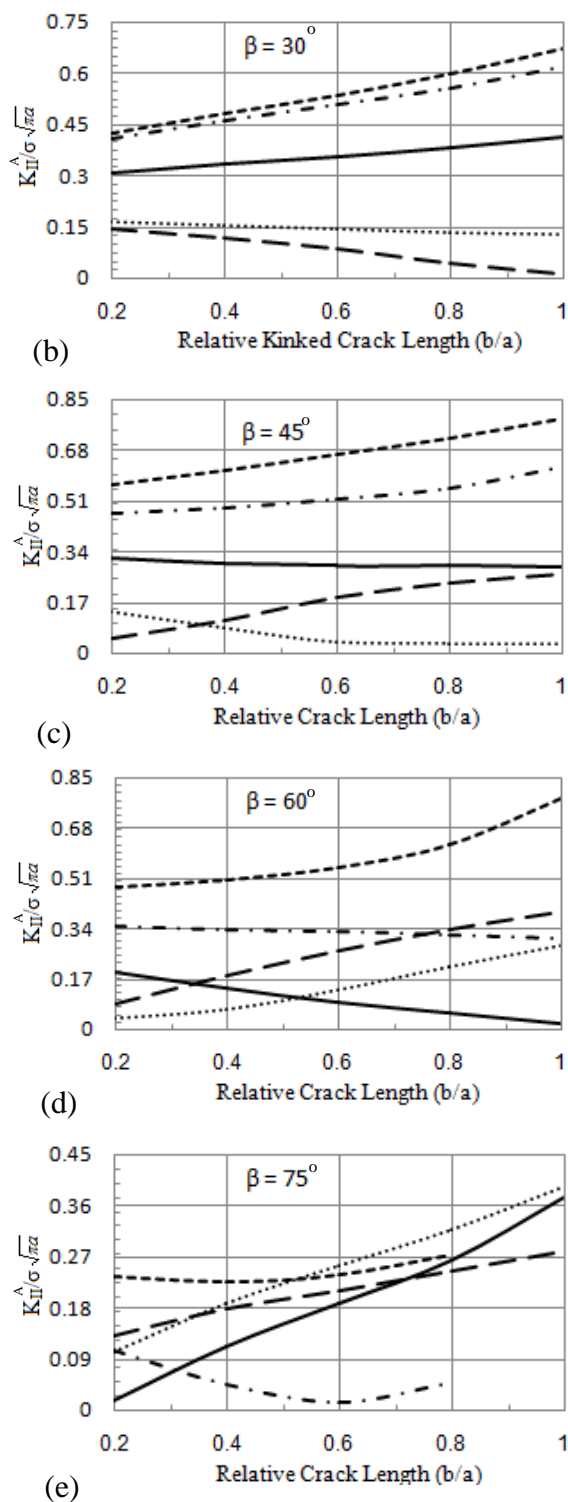
Figure(8) Deformed and Undeformed Edge for an Corner Cracked Plate

4.2 Central Kinked Cracked Plates

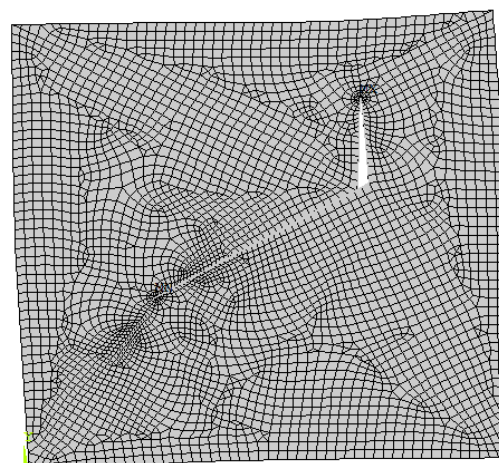
Figure(9) shows the variation of $K_{II}^A / \sigma \sqrt{\pi a}$ with relative crack length (b/a) for different kink angles (α) of the five considered crack orientation (β), where K_{II}^A is the mode II SIF at crack tip A, see figure (3b). In order to study the effect of the crack kink angle and extension on the mode II SIF, central kinked cracked plate case is considered. As exposed in this case, $K_{II}^A / \sigma \sqrt{\pi a}$ is slightly decreased when $(\alpha + \beta) = 90^\circ$, figures (9a-9e), and it is significantly decreases when $(\alpha + \beta) = 105^\circ$, figure(9c-9e). Also, figure(9) shows that there was considerable increase in $K_{II}^A / \sigma \sqrt{\pi a}$ when $(105^\circ < (\alpha + \beta) < 90^\circ)$. This behavior can be explained by the relation between loading direction and crack face. As the kinked crack becomes parallel to the loading direction, it opens leading to a decrease in mode II SIF and increase in Mode I SIF at tip A. So, figure(10) has been plotted to demonstrate how the crack can open in this case. Furthermore, it is noted that when $\beta = 75^\circ$ and $(b/a) > 0.6$ at $\alpha = 15^\circ - 30^\circ$ there is a slight increase in $K_{II}^A / \sigma \sqrt{\pi a}$ since the kinked crack length is very close to the plate boundary. Consequently, the case of $b/a = 1$ is not taken because of intersection between crack and plate boundary.



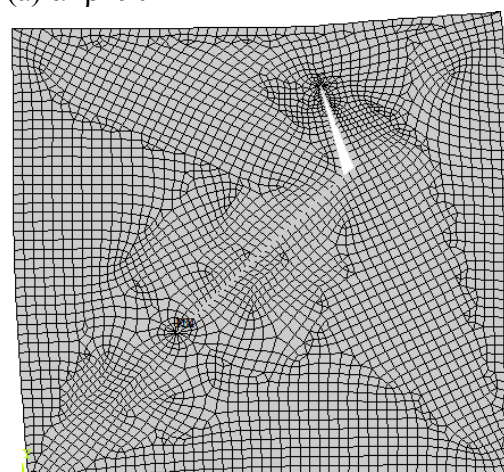
(a) (Continued)



Figure(9) Normalized Mode II SIF Versus Relative Kinked Crack Length for Different Kink Angle and Crack Orientation



(a) $\alpha + \beta = 90^\circ$



(b) $\alpha + \beta = 105^\circ$

Figure(10) Deformed Shape of Open Crack For Kinked Cracked Plate

5- Conclusions

The analysis and determination of second mode stress intensity factor (K_{II}) of cracked plates under uniaxial compression is presented in this study. Two cases have been investigated, diagonal cracked plates and central kinked cracked plates. The obtained results can be summarized as follows:

- (1) When the crack moves from the plates corner to the plate centre, a significant reduction in the mode II SIF exists.
- (2) The corner cracked plates have the highest mode II SIF, so can be

considered more liable to fracture than the other cracked plates.

- (3) Mode II SIF increases with increasing crack orientation and decreases after reaching a maximum value. Consequently, the case of the plate with a crack orientation $\beta=45^\circ$ shows intermediate behavior for diagonal cracked plate.
- (4) There is a decrease in mode II SIF at $\alpha+\beta=90^\circ$ or 105° . On the other hand, when $105^\circ < \alpha+\beta < 90^\circ$ there is an increase in mode II SIF.

References

- [1] Banks-Sills L, Sherman D. Comparison of methods for calculating stress intensity factors with quarter-point elements. *International Journal of Fracture* 1986;32:127–40.
- [2] Lim IL, Johnston IW, Choi SK. Comparison between various displacement-based stress intensity factor computation techniques. *International Journal of Fracture* 1992;58:193–210.
- [3] Mukhopadhyay NK, Maiti SK, Kakodkar A. A review of SIF evaluation and modeling of singularities in BEM. *Computer Mechanics* 2000;25:358–75.
- [4] Murthy KSRK, Mukhopadhyay M. Unification of stress intensity factor (SIF) extraction methods with an h-adaptive finite element scheme. *Communications in Numerical Methods of Engineering*. 2001;17:509–20.
- [5] Murakami Y. *Stress intensity factors handbook*. England: Pergamon; 1987.
- [6] Tada H, Paris PC, Irwin GR. *The stress analysis of cracks handbook*. New York: ASME; 2000.
- [7] Jukka Tuhkuri. Dual boundary element analysis of closed cracks. *International Journal for Numerical Methods in Engineering* 1997; 40:2995-3014.
- [8] Ashby M. F. and Sammis C. G. The damage mechanics of brittle solids in compression. *Pure and Applied Geophysics* 1990;133;3:489-521.
- [9] Carpinteri A., Scavia C. and Yang G. P. Microcrack propagation, coalescence and size effects in compression. *Engineering Fracture Mechanics* 1996; 54;3:335-347.
- [10] Jian Niu and Mao S. Wu. Analysis of asymmetric kinked cracks of arbitrary size, location and orientation – Part I. Remote compression. *International Journal of Fracture* 1998;89: 19–57.
- [11] Antonio Bobet. The initiation of secondary cracks in compression. *Engineering Fracture Mechanics* 2000;66:187-219.
- [12] Lee S. and Ravichandran G. Crack initiation in brittle solids under multiaxial compression. *Engineering Fracture Mechanics* 2003;70:1645–1658.
- [13] Chen Shun-yun et. al. Application of caustic method to determining stress intensity factor of compressive shear crack. *ACTA SEISMOLOGICA SINICA* 2005;18;4:483-489.
- [14] Akihito Saimoto, Akira Toyota and Yasufumi Imai. Compression induced shear damage in brittle solids by scattered microcracking. *International Journal of Fracture* 2009;157:101–108.
- [15] Heekwang Lee and Seokwon Jeon. An experimental and numerical study of fracture coalescence in pre-cracked specimens under uniaxial compression. *International Journal of Solids and Structures* 2011;48:979–999.
- [16] Zhu Z, Ji S and Xie H. An improved method of collocation for the problem of crack surface subjected to uniform load. *Engineering Fracture Mechanics* 1996;54;5:731–41.
- [17] Zhu Z, Xie H and Ji S. The mixed boundary problems for a mixed mode

- crack in a finite plate. *Engineering Fracture Mechanics* 1997;56;5:647–55.
- [18] Zhu Z. et. al. Stress intensity factor for a cracked specimen under compression. *Engineering Fracture Mechanics* 2006;73: 482–489.
- [19] Chau K.T. and Wang Y.B. Singularity analysis and boundary integral equation method for frictional crack problems in two-dimensional elasticity. *International Journal of Fracture* 1998;90:252-274.
- [20] Tsung-Chieh Chen and Wen-Hwa Chen. Frictional contact analysis of multiple cracks by incremental displacement and resultant traction boundary integral equations. *Engineering Analysis with Boundary Elements* 1998;21: 339-348.
- [21] Isaksson P. and Stahle P. Crack kinking under high pressure in an elastic-plastic material. *International Journal of Fracture* 2001;108: 351–366.
- [22] Isaksson P. and Stahle P. A directional crack path criterion for crack growth in ductile materials subjected to shear and compressive loading under plane strain conditions. *International Journal of Solids and Structures* 2003;40: 3523–3536.
- [23] Hammouda M.M.I. , Fayed A.S. and Sallam H.E.M. Mode II stress intensity factors for central slant cracks with frictional surfaces in uniaxially compressed plates. *International Journal of Fatigue* 2002;24:1213–1222.
- [24] Hammouda M.M.I. , Fayed A.S. and Sallam H.E.M. Stress intensity factors of a shortly kinked slant central crack with frictional surfaces in uniaxially loaded plates. *International Journal of Fatigue* 2003;25; 283–298.
- [25] Hammouda M.M.I. , Fayed A.S. and Sallam H.E.M. Stress intensity factors of a central slant crack with frictional surfaces in plates with biaxial loading. *International Journal of Fracture* 2004;129:141–148,.
- [26] Hammouda M.M.I. , Fayed A.S. and Sallam H.E.M. First crack initiation angle of central slant crack in plates under compression-tension biaxial loading. *Journal of Al Azhar University Engineering Sector* 2008; 3; 6:13-26.
- [27] Xian-Fang Li ,Guang-Lian Liu and Kang Yong Lee . Effects of T-stresses on fracture initiation for a closed crack in compression with frictional crack faces. *International Journal of Fracture* 2009;160:19–30.